Molecular Crystals and Liquid Crystals

ISSN: 1542-1406 (Print) 1563-5287 (Online) Journal homepage: http://www.tandfonline.com/loi/gmcl20

O-hydroxy Schiff Bases Derived from 2-Hydroxy-4-methoxy Benzaldehyde: Synthesis, X-Ray Studies and Hydrogen Bonding Attributes

A. L. Amrutha Kala, Nanishankar V. Harohally, S. Naveen, M. Ramegowda & N. K. Lokanath

To cite this article: A. L. Amrutha Kala, Nanishankar V. Harohally, S. Naveen, M. Ramegowda & N. K. Lokanath (2016) O-hydroxy Schiff Bases Derived from 2-Hydroxy-4-methoxy Benzaldehyde: Synthesis, X-Ray Studies and Hydrogen Bonding Attributes, Molecular Crystals and Liquid Crystals, 629:1, 146-157, DOI: 10.1080/15421406.2015.1107814

To link to this article: http://dx.doi.org/10.1080/15421406.2015.1107814

MOLECULAR CRYSTALS AND LIQUID CRYSTALS
2016, VOL. 629, 146–157
http://dx.doi.org/10.1080/15421406.2015.1107814

Taylor & Francis
Taylor & Francis Group

O-hydroxy Schiff bases derived from 2-hydroxy-4-methoxy benzaldehyde: Synthesis, x-ray studies and hydrogen bonding attributes

A. L. Amrutha Kala[a,b], Nanishankar V. Harohally[a], S. Naveen[c], M. Ramegowda[d], and N. K. Lokanath[b]

[a]Food Safety and Analytical Quality Control Laboratory Building, CSIR-CFTRI, Mysore, Karnataka, India; [b]Department of Studies in Physics, University of Mysore, Manasagangothri, Mysore, Karnataka, India; [c]Vijnana Bhavana, Manasagangothri, University of Mysore, Mysore, Karnataka, India; [d]Government College (Autonomous) Mandya, Karnataka, India

ABSTRACT

The o-hydroxy Schiff bases consisting of N′-[(Z)-(2-hydroxy-4-methoxyphenyl)methylidene]pyridine-4-carbohydrazide and N′-[(Z)-(2-hydroxy-4-methoxyphenyl)methylidene]pyridine-3-carbohydrazide were prepared by reaction of isonicotinic acid hydrazide and nicotinic acid hydrazide by employing 2-hydroxy-4-methoxy benzaldehyde. The spectroscopic techniques, X-ray crystal structure determination as well as DFT calculations have been carried out to shed light on the nature of hydrogen bonding. The both experimental and theoretical investigations demonstrate the presence of intramolecular neutral hydrogen bonding (enol-imine type) in these molecules.

KEYWORDS

Hydrogen bonding; NMR; *o*-hydroxy Schiff base; X-ray

Introduction

Schiff bases are well-known ligands for assembling metal complexes and are accomplished by reaction of aromatic aldehydes and ketones with primary amines via elimination of H_2O [1]. Among these important family of ligands, *o*-hydroxy Schiff bases are formed by substituted-2-hydroxy salicylaldehydes or napthaldehydes with primary amines. The *o*-hydroxy Schiff bases have attracted attention due to formation of interesting hydrogen bonding as a consequence of pseudo-aromatic chelate ring formation [[2–5]. Further, hydrogen bonding in *o*-hydroxy Schiff bases has attracted pivotal importance due to its relevance to biological processes [6–8]. The *o*-hydroxy Schiff bases can in principle exhibit two tautomeric form consisting of enol-imine and keto-imine form. The former tautomeric form exhibit neutral hydrogen bonding, whereas the latter in principle display neutral hydrogen bonding or ionic hydrogen bonding (zwitter ionic form of keto-imine form) [5]. The hydrogen bonding in *o*-hydroxy Schiff bases have been thoroughly investigated using solution as well as solid state NMR, IR spectroscopy, X-ray, and neutron diffraction [9–12]. There is current focus

CONTACT Nanishankar V. Harohally nani.shankar@gmail.com N. K. Lokanath lokanath@physics.uni-mysore.ac.in
Department of Studies in Physics, Mysore University, Manasagangothri, Mysore 570006, Karnataka, India.
Color versions of one or more of the figures in the article can be found online at www.tandfonline.com/gmcl.

on effect of substituents on the nature of hydrogen bonding in these classes of *o*-hydroxy Schiff bases. In view of current attention, our aim was to accomplish *o*-hydroxy Schiff bases by employing hydrazide instead of a regular amine. Toward this goal, we utilized readily available isonicotinic acid hydrazide and nicotinic acid hydrazide, in addition, we employed the unusual flavour molecule 2-hydroxy-4-methoxybenzaldehyde (HMBA) for the formation of *o*-hydroxy Schiff bases. In this paper, we discuss synthesis of these *o*-hydroxy Schiff bases as well as X-ray structure and hydrogen bonding attributes from spectroscopic, X-ray, and DFT studies.

Experimental

Isonicotinic acid hydrazide and nicotinic acid hydrazide and 2-hydroxy-4-methoxybenzaldehyde were procured of Sigma-Aldrich. NMR spectra were recorded on a Bruker Avance instrument (400 MHz for ^{1}H and 100 MHz for ^{13}C{H} experiments). Proton and carbon chemical shifts are given relative to residual solvent signal for dmso-d_6 (2.50 ppm for ^{1}H and 39.52 for ^{13}C). NMR spectral assignments for compounds **1** and **2** were accomplished by employing ^{1}H, ^{13}C, HSQC (heteronuclear single quantum coherence), HMBC (heteronuclear multiple bond correlation), DEPT (distortionless enhancement by polarization transfer) experiments. Mass spectra were recorded in the Q-TOF ULTIMA instrument of Waters Corporation in the ESI positive mode. The IR spectra was recorded utilizing Thermo FT-IR instrument.

X-Ray crystal structure determination

White rectangle (I)- and white needle (II)-shaped single crystals of dimensions 0.27 × 0.26 × 0.25 mm and 0.30 × 0.28 × 0.26 mm, respectively, were chosen carefully for X-ray diffraction studies. X-ray intensity data were collected at temperature 296 K on a Bruker Proteum2 CCD diffractometer with X-ray generator operating at 45 kV and 10 mA, using CuK_{α} radiation of wavelength 1.54178 Å . Data sets were collected with different settings of φ (0° and 90°), keeping the scan width of 0.5°, exposure time of 5 s, and the sample to detector distance was 45.10 mm. The compounds **1** and **2** were crystallized in the monoclinic and triclinic space group, respectively. The complete intensity data sets were processed using *SAINT PLUS* [13]. The structures were solved by direct methods and refined by full-matrix least squares method on F^2 using *SHELXS* and *SHELXL* programs [14]. All the non-hydrogen atoms were revealed in the first difference Fourier map itself. All the hydrogen atoms were positioned geometrically (C–H = 0.93 Å , O–H = 0.82 Å) and refined using a riding model with U_{iso}(H) = 1.2 U_{eq}(C,N) and U_{iso}(H) = 1.5 U_{eq}(O). After several cycles of refinement, the final difference Fourier map showed peaks of no chemical significance and the residuals saturated to 0.0331 and 0.0431 for (I) and (II), respectively. The geometrical calculations were carried out using the program *PLATON* [15]. The molecular and packing diagrams were generated using the software *MERCURY* [16]. The details of the crystal data and structure refinement are given in the supporting information.

Computational details

Ground-state optimization of the molecules have been performed by using B3LYP [17–19] hybrid function with cc-pVDZ [20] basis set at a DFT level [21–26]. TDDFT [27–35] is used for transition energy calculation within a DFT framework using same function and

basis set. Based on optimized ground state geometries in DMSO solvent using CPCM-B3LYP/cc-pVDZ [36–37] model, the transition energies were calculated by TD-CPCM-B3LYP/cc-pVDZ method [38]. All calculations were performed using GAMESS-US software suit [39,[40].

N′-[(Z)-(2-hydroxy-4-methoxyphenyl)methylidene]pyridine-4-carbohydrazide (1)

In a round bottom flask connected to a Liebig condenser set up having a magnetic stir bar, isonicotinic acid hydrazide (1.37 g, 10 mmol) was dissolved in methanol (10 mL). To this solution was added 2-hydroxy-4-methoxybenzaldehyde (1.52 g, 10 mmol). The reaction mixture was refluxed with stirring for 2 hr till precipitate is observed. Then, the precipitate was filtered and washed thoroughly with methanol and followed by ether. The crystals were grown by dissolving the compound in excess methanol followed by slow evaporation of methanol solvent.

Yield = 2.49 g, 85%. ESI-MS Positive mode $(M+H)^+$ *m/z* 294.1808, exact mass $(M+H)^+$ 294.1552. ^{1}H NMR δ 3.77 (s, 3H, CH_3)), 6.50 (d, 1H, CH(11), 6.53 (d, 1H, CH(5)), 7.48 (d, 1H, HC(6)), 7.83. (*d*, 1H, $J = 5.9$ Hz, HC(11)), 8.57(*s* 1H, HC(8)), 8.79 (*d*, 1H, $J = 5.6$ Hz, HC(12)), 8.79 (*d*, 1H, $J = 5.6$ Hz, HC(13)), 7.83. (*d*, 1H, $J = 5.9$ Hz, HC(14)) 11.42 (bs,1H, NH),12.2 (bs,1H, OH). ^{13}C NMR δC 150.35 (C-14), 121.45 (C-13), 121.45 (C-12), 150.35 (C-11), 140.05 (C-10), 162.36 (C-9), 149.60 (C-8), 55.35 (C-7), 131.02 (C-6), 106.61 (C-5), 159.45 (C-4), 101.17 (C-3), 161.08 (C-2), 111.70 (C-1).

N′-[(Z)-(2-hydroxy-4-methoxyphenyl)methylidene]pyridine-3-carbohydrazide (2)

The compound 2 was prepared similar to compound **1** by utilizing nicotinic acid hydrazide and 2-hydroxy-4-methoxybenzaldehyde.

Yield = 2.52 g, 86%. ESI-MS Positive mode $(M+H)^+$ *m/z* 294.1808, exact mass $(M+H)^+$ 294.1552. ^{1}H NMR δ 3.77 (*s*, 3H, CH_3)), 6.50 (*s*, 1H, CH(3), 6.53 (*d*, 1H, $J = 8.5$ Hz, CH(5)), 7.46 (*d*, 1H, $J = 8.5$ Hz, HC(6)), 8.55 (*s*, 1H, CH(8), 7.57. (dd, 1H, $J = 4.8$ Hz, $J = 7.9$ Hz, HC(11)), 8.26 (d, 1H, $J = 7.9$ Hz, HC(12)), 8.76 (*d*, 1H, $J = 4.3$ Hz, HC(13)), 9.07.(*s*, 1H, HC(14)) 11.49 (bs,1H, NH),12.15 (bs,1H, OH). ^{13}C NMR δC 148.56 (C-14), 152.36 (C-13), 135.38 (C-12), 123.63 (C-11), 128.76 (C-10), 162.26 (C-9), 149.17 (C-8), 55.33 (C-7), 131.08 (C-6), 106.57 (C-5), 159.43 (C-4), 101.18 (C-3), 161.19 (C-2), 111.71 (C-1).

Results and discussion

O-hydroxy Schiff bases were synthesized by employing 2-hydroxy-4-methoxybenzaldehyde with isonicotinic acid hydrazide and nicotinic acid hydrazide under reflux conditions in methanol solvent (Fig 1).

The reaction was smooth and yield was quantitative (85–86%). Both compounds were found to be sparingly soluble in methanol and completely soluble in DMSO. The accomplished compounds were characterized by Mass, IR, and NMR spectroscopic techniques. The crystals were prepared by slow evaporation of solution of respective compounds in excess methanol solvent.

Spectroscopic characterization

The NMR spectra were recorded in dmso-d_6. The ^{1}H NMR of accomplished compounds exhibited typical peaks corresponding to the Schiff bases of isonicotinic acid hydrazide and

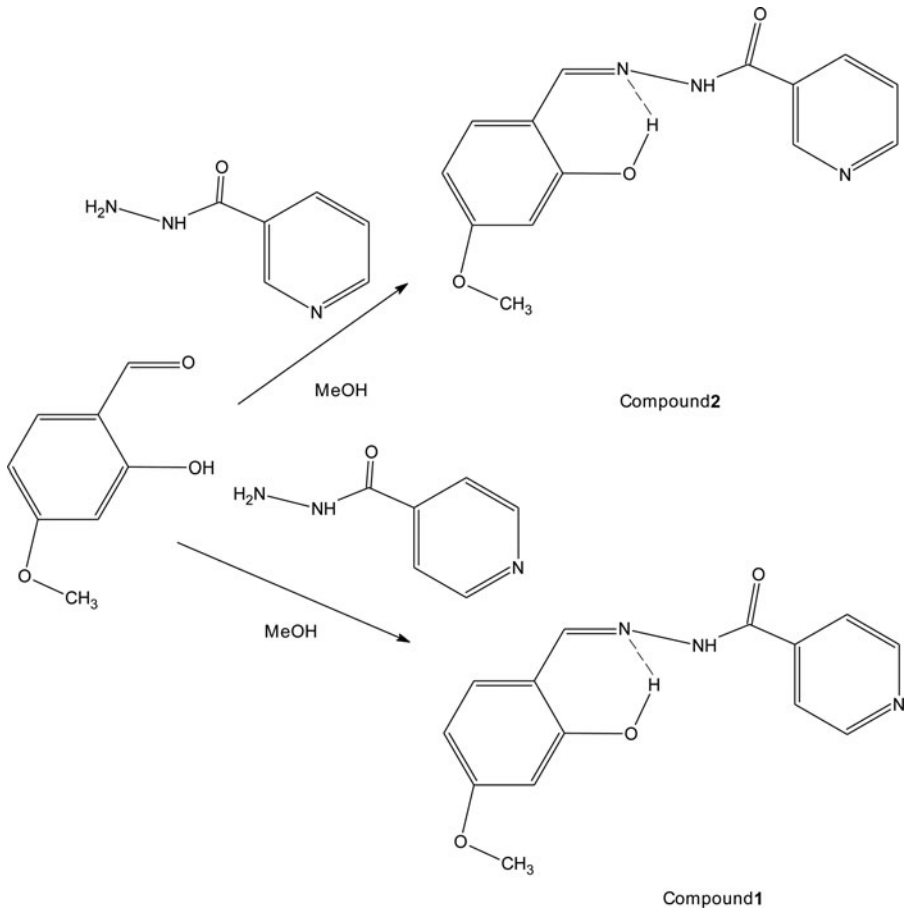

Figure 1. Synthesis of O-hydroxy Schiff bases; solvent and reaction conditions: MeOH and 30°C, reflux for 2 hr.

nicotinic acid hydrazide. The proton NMR of compounds **1** and **2** displayed proton attached imine group in the range 8.0–9.5 ppm, whereas the ^{13}C NMR exhibited the peaks in the range 150–170 ppm. The ^{1}H NMR spectrum of HMBA portion was observed at 6.50, 6.53, and 7.48 ppm for compound **1**, whereas for the compound **2** peaks at 6.50, 6.53, and 7.48 ppm confirmed the typical peak pattern due to HMBA. The pyridine moiety of isonicotinic acid hydrazide attached to compound **1** was further confirmed by observing peaks at 7.83 and 8.79 ppm in ^{1}H NMR, whereas pyridine moiety attached to compound **2** was confirmed with four distinct peaks at 7.57, 8.26, 8,76, and 9.07 ppm.

The high-resolution mass spectral analyses clearly demonstrated the molecular formula of the compounds via observation of molecular ions for compound **1** at 272.1634 and 294.0826 and for the compound **2** at 272.1500 and 294.0687 corresponding to MH^+ and MNa^+ molecular ions, respectively.

The IR spectrum clearly exhibited broad bands for compound **1** and **2** at 3430 cm^{-1} and 3379 cm^{-1} attributable to O–H stretch. On the other hand, medium intensity medium bands at 3317 and 3207 cm^{-1}, respectively, clearly marked the presence of N-H stretch. The C–H band observed at 3036 and 3072 cm^{-1}, respectively, indicates the presence of aromatic ring. The two weak bands just below 3000 cm^{-1} at 2974 and 2840 cm^{-1}, respectively, for compound

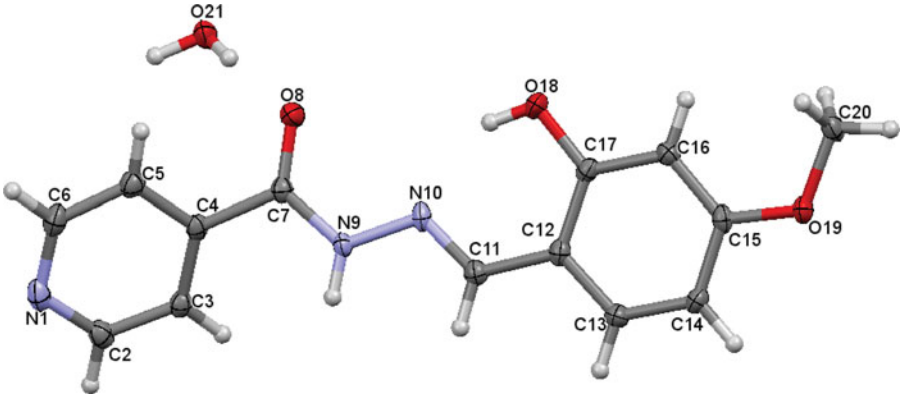

Figure 2. ORTEP diagram of compound 1.

1 represented asymmetric and symmetric stretch of methyl group, there by confirming methyl group. The strong bands at 1673 and 1659 cm^{-1}, respectively, confirmed the presence of C = O group for compound **1** and **2**, whereas weaker bands at 1620 and 1626 cm^{-1}, respectively, for compounds **1** and **2** represented the C=N group. The aromatic ring modes were observed at 1591 and 1604 cm^{-1}, respectively, for compounds **1** and **2**. A medium intensity band at 1322 and 1355 cm^{-1}, respectively, are attributed to O–H in plane bend, whereas the bands at 1248 and 1226 cm^{-1}, respectively, are attributed to C–N stretch.

Hydrogen bonding by spectroscopic techniques

The IR spectra recorded for compounds **1** and **2** clearly demonstrate the presence of hydrogen bonded O-H group (2-hydroxy group), which displays band due to O-H stretching at 3430 and 3379 cm^{-1}, respectively, which is typical of hydrogen bonded O-H as compared to phenolic naked O-H stretching frequency of 3500 cm^{-1}.

The proton NMR of the compounds **1** and **2** evidently confirms the hydrogen bonding (δ = 12–13 ppm); however, the ^{1}H NMR spectra cannot distinguish the nature of hydrogen bonding either to be ionic or neutral. [2] On the other hand, ^{13}C NMR spectral attributes of C_2-OH of compounds **1** and **2** (δ = 161.08 for C_2 of compound **1** and δ = 161.19 for C_2 of compound **2**) clearly demonstrated the downfield shift of carbon signals indicating carbonyl

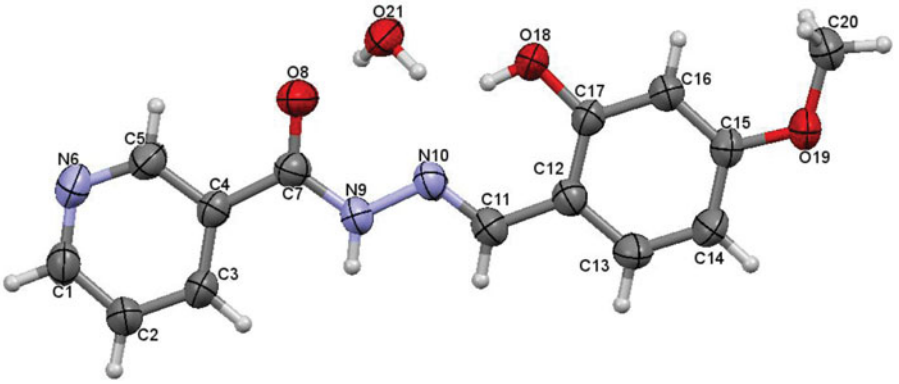

Figure 3. ORTEP diagram of Compound 2.

Table 1. Selected bond distances and bond angles for compound 1 and compound 2.

Compound 1 Bond lengths		Compound 2 Bond lengths	
N1-C3	1.3411(19)	C1-N6	1.331(2)
N1-C6	1.3415(19)	C5-N6	1.334(2)
N9-N10	1.3812(15)	N9-N10	1.3791(18)
N10-C11	1.2868(17)	N10-C11	1.286(2)
C7-N9	1.2320(17)	C7-N9	1.350(2)
C7-O8	1.2320(17)	C7-O8	1.2273(19)
C11-C12	1.4441((18)	C11-C12	1.444(2)
C12-C13	1.4025(19)	C12-C13	1.405(2)
C12-C17	1.4088(19)	C12-C17	1.399(2)
C17-018	1.3509(16)	C17-018	1.3566(18)
Bond angles		Bond angles	
C2-N1-C6	117.01(12)	C1-N6-C5	116.32(14)
C4-C7-O8	121.52(12)	C4-C7-O8	120.61(14)
C7-N9-N10	119.36(11)	C7-N9-N10	118.73(13)
N10-C11-C12	121.97(12)	N10-C11-C12	121.37(14)
C12-C17-O18	121.86(12)	C12-C17-O18	121.93(14)
C16-C17-O18	117.50(12)	C16-C17-O18	117.06(14)
C15-O19-C20	117.68(10)	C15-O19-C20	118.63(12)

kind of environment corroborating with enol form and neutral hydrogen bonding. Attempts to get ^{15}N NMR for the compounds were not successful due to inherent limitation due to solubility issues.

X-Ray crystal structure determination

The ORTEP diagram of the compound **1** and **2** are shown in Fig 2 and Fig 3 respectively. The selected bond distances and bond angles for the compounds are shown in Table 1. Intermolecular and intramolecular hydrogen bonding distances for compounds **1** and **2** are represented in Table 2 and Table 3. The conformation of the molecules can be described by the dihedral angles between the aryl ring and the pyridine ring and the torsions defining the conformation of the chain bridging the two rings. In *N*'-[(*Z*)-(2-hydroxy-4-methoxyphenyl)methylidene]pyridine-4-carbohydrazide (**1**), the dihedral angle between the two aryl rings is 36.24(6)° which is significantly higher than the value of 2.08(8)° observed for *N*'-[(*Z*)-(2-hydroxy-4-methoxyphenyl)methylidene]pyridine-3-carbohydrazide (**2**). This can directly be attributed to the steric hindrance caused by the substitutional change in the pyridine ring. The torsion angles defining the conformation of the chain bridging the two aryl rings in (I) have values C4-C7-N9-N10 = −172.07(11)°, C12-C11-N10-N9 = −176.57(11)° and C7-N9-N10-C11 = 176.80(11)°. And similar values of torsion angles are observed in the

Table 2. Geometric parameters and symmetry codes for hydrogen bonds, intra- and intermolecular contacts (Å , deg) in compound 1.

D–H …A	D–H	H …A	D …A	D–H …A
N9-H9 …O21^{i}	0.86	2.05	2.8963(15)	169
O21-H22 …N1^{ii}	0.89(2)	1.95(2)	2.8319(16)	177(2)
C3-H3 …O21^{i}	0.93	2.60	3.2370(17)	126
C6-H6 …O19^{iii}	0.93	2.55	3.4701(16)	170
C20-H20A …O8^{iv}	0.96	2.48	3.4074(17)	163
O18-H18 …N10	0.82	1.93	2.6552(15)	147
O21-H21 …O8	0.88(2)	2.02(2)	2.8903(14)	174(2)

(i) 1−*x*, −1/2+*y*,1/2−*z*; (ii) 1−*x*,1−*y*,1−*z*; (iii) *x*,*y*,1+*z*; (iv) *x*,3/2−*y*, −1/2+*z*.

Table 3. Geometric parameters and symmetry codes for hydrogen bonds, intra- and intermolecular contacts (Å , deg) in compound 2.

D–H …A	D–H	H …A	D …A	D–H …A
N9-H9 …O21^{i}	0.86	2.09	2.922(2)	164
O21-H21A …N6^{ii}	0.90(3)	2.07(3)	2.957(2)	166(2)
C3-H3 …O21^{i}	0.93	2.43	3.345(2)	167
C11-H11 …O21^{i}	0.93	2.60	3.372(2)	141
C20-H20B …O19^{iii}	0.96	2.56	3.327(2)	136
O18-H18 …N10	0.82	1.94	2.6547(19)	146
C5-H5 …O8	0.93	2.40	2.755(2)	102

(i) −1+*x*,*y*,*z*; (ii) *x*, −1+*y*,*z*; (iii) −*x*, −1−*y*,1−*z*.

compound II, C4-C7-N9-N10 = 178.11(12)°, C12-C11-N10-N9 = −178.56(13)°, and C7-N9-N10-C11 = −176.53(14)°. The methoxy group lies in the plane of the phenyl ring as indicated by the torsion angle values of 2.32(18)° and 0.8(2)° for the chain C16-C15-O19-C20 in the molecules of I and II, respectively. In the molecule I, the crystal structure features extensive strong and weak hydrogen bonding. The molecules are linked to one another via water molecules through strong N9-H9 …O21 and O21-H21 …O8 hydrogen bonds forming chains along *a* axis (Figs. 2 and 3). The parallel chains are interlocked through strong O21-H22 …N1 hydrogen bonds. The crystal structure is further stabilized by weak C3-H3 …O21, C6-H6 ….O19, and C20-H20A O8 hydrogen bonds and π-π stackings (involving the centroid of the pyridine ring). In the compound **2**, the molecule are linked to one another via water molecules through strong N9-H9 …O21 and O21-H21 …O8 hydrogen bonds forming chains along c axis (Fig 4 and Fig 5). The parallel chains are interlocked through strong O21-H21a …N6 hydrogen bonds. The crystal structure is further stabilized by weak C3-H3 …O21, C11-H11 ….O21, and C20-H20b …O19 hydrogen bonds and three pi …pi stacking interactions – cg1 …cg1 (3.7963 Å), cg1 …cg2 (3.7179 Å), and cg2 …cg2 (3.9415 Å) (cg1 and cg2 are the centroids of the aryl ring and the pyridine ring).

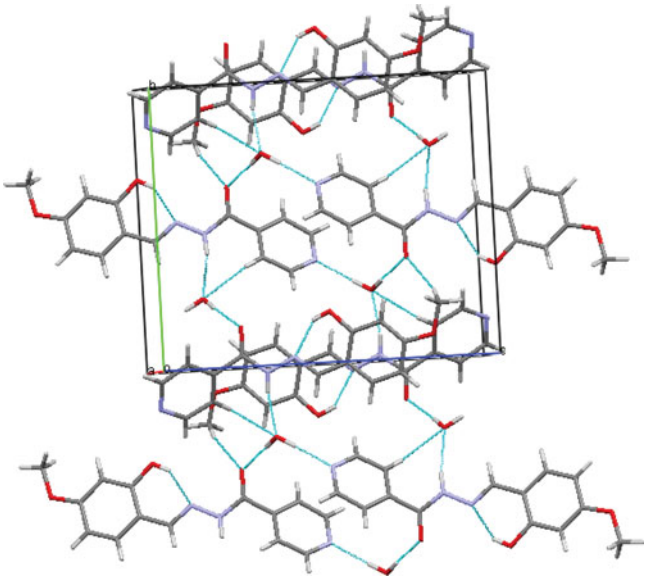

Figure 4. Packing Diagram for Compound 1.

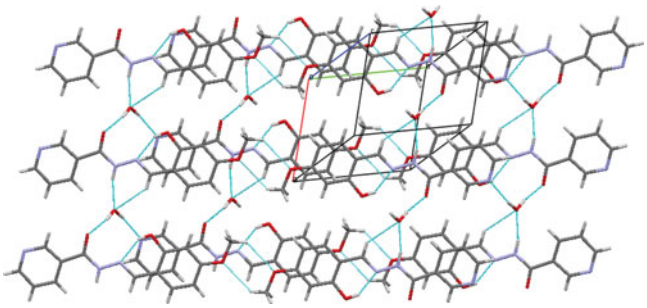

Figure 5. Packing Diagram for Compound 2.

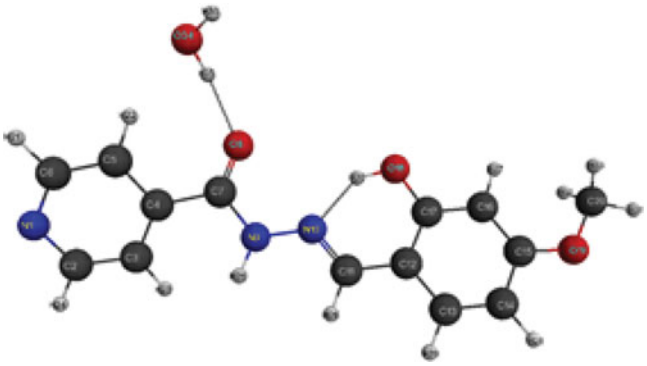

Figure 6. Optimized structure of compound 1.

Optimized structure, MOs, and electronic excitation energies

Figures 6 and 7 depicts the ground state optimized structure of the molecules and their geometrical parameters are listed in supporting information. The HOMO and LUMO energies for the molecules **1** and **2** have been calculated by the B3LYP/cc-pVDZ method and the calculation reveals that there were 71 occupied and 274 unoccupied molecular orbitals. The frontier molecular orbitals (MOs) of the compounds are depicted in Fig. 8.

The excited states of the molecules are mainly due to the orbital transition from HOMO to LUMO, which involves the intramolecular charge redistribution from the phenyl ring C12/C13/C14/C15/C16/C17 and N9-N10-C11 to the pyridine ring N1/C2/C3/C4/C5/C6 and carbonyl group C=O. Furthermore, it has been confirmed by the population analysis that the

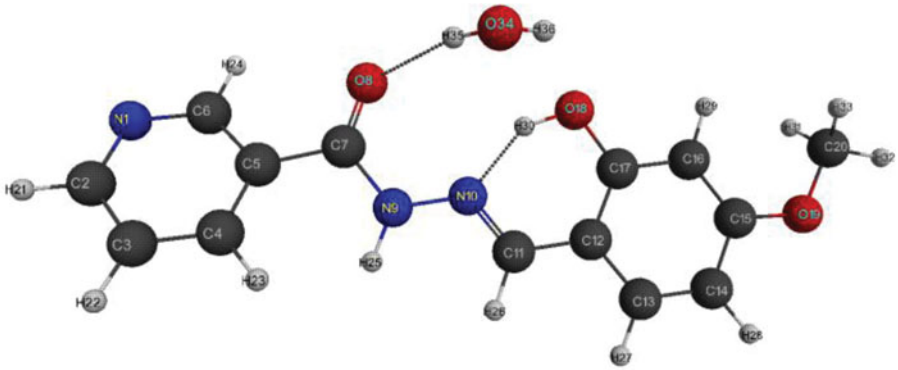

Figure 7. Optimized Structure of compound 2.

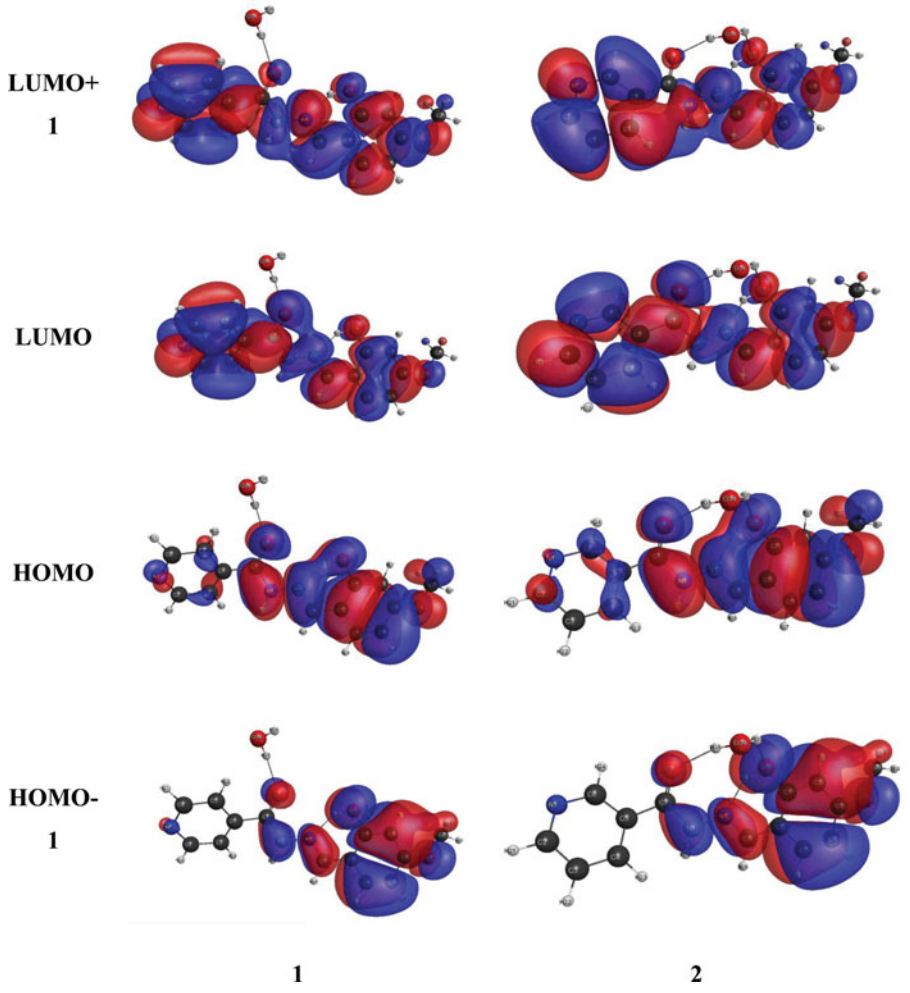

Figure 8. Occupied and virtual molecular orbitals responsible for the electronic absorption spectrum of the molecule.

Mulliken (electronic) charge is decreased on phenyl ring and on pyridine ring it is increased (see Table 4). Also charge on N9-N10-C11 chain is decreased, whereas on carbonyl group Mulliken charge is increased. Thus, the exited states of the molecule may be an intramolecular charge-transfer (ICT) state.

Table 4. The Mulliken charges (*e* units) on various groups of the molecules at S_0 and S_1 states.

	1		2	
Groups	S_0	S_1	S_0	S_1
Pyridine ring N1/C2/C3/C4/C5/C6	− 0.065	− 0.261	0.051	− 0.137
C7 = O8	− 0.064	− 0.140	− 0.050	− 0.129
N9-N10-C11 chain	− 0.083	− 0.047	− 0.083	− 0.041
phenyl ring C12/C13/C14/C15/C16/C17	0.198	0.329	0.208	0.339
Hydroxyl group	− 0.171	− 0.119	− 0.217	− 0.164
Methoxyl group	− 0.149	− 0.140	− 0.149	− 0.138

Table 5. The Mulliken charges (*e* units) on N9, N10, C11, O18, and H30 atoms at S_0 state.

Molecule	N9	N10	C11	O18	H30
1	−0.079	−0.176	0.1721	−0.171	0.1568
2	−0.082	−0.179	0.1781	−0.217	0.1826

The TDDFT/PCM calculations of the molecules **1** and **2** produce the intense absorption wavelengths in DMSO solvent at 335.10, 378.92, 380.90, and 367.3 nm, respectively (Fig. 8) (supporting information).

Molecular electrostatic potential

Molecular electrostatic potential (MEP) provides a visual method to predict reactive sites for electrophilic and nucleophilic attack for the molecules. The different values of the electrostatic potential at the surface were represented by different colors, and the color code of these maps was in the range from −0.001 a. u. (deepest red) to 0.001 a. u. (deepest blue). The negative (red color) regions of MEP were related to electrophilic reactivity and the positive (blue color) ones to nucleophilic reactivity as shown in Fig. 8. From the MEP, it was evident that in all molecules most electrostatic potential regions (red) were mainly localized over N1, O8, N10, O18, and O19 atoms showing the most favourable sites for electrophilic attack. Meanwhile, a maximum positive region (blue) is localized over heterocyclic ring (except N1), which are indicating possible sites for nucleophilic attack. C14 and C16 atoms of the phenyl ring also shows tendency for electrophilic attack

Hydrogen bonding by x-ray crystal structure

The C=O bond distances for compounds **1** and **2** are 1.355 and 1.357 Å , respectively, whereas C–N bond distances for the compounds **1** and **2** are, respectively, 1.285 and 1.276 Å . These distances are comparable to enols forms of salicylideneanilines with reported distance of C=O in the range 1.340–1.351 Å and C–N distances in range 1.264–1.286 Å [3]. On the other hand, the intramolecular hydrogen bond is observed between the hydrogen of ortho hydroxyl group and nitrogen of imine is represented by the O…N distances which are respectively 2.655 and 2.655 Å for compounds **1** and **2**. These bond distances are slightly higher to enol forms of 4-methoxy salicylideneanilines having the range 2.58–2.59 Å and are similar to keto form of 4-methoxy salicylideneanilines having distances 2.63–2.65 Å [3]. Apart from these, the C–C bond distance for compound **1** (C17–C12) is 1.405 Å , whereas for the compound **2**, it is 1.399 Å . The C–C bond distances connecting aromatic ring and aldimine carbon distances are 1.453 and 1.444 Å , respectively, for **1** and **2**. The former distances indicate typical of aromatic C–C bond distances and latter appreciably deviates from aromatic C–C bond distances indicating enol form to be existing.

Table 6. OH bond length, HB length, and angles from DFT calculation.

Molecule	O18-H30(Å)	O18-H30—N10(°)	H30—N10(Å)
1	0.993	144.8	1.746
2	0.998	147.4	1.690

Table 7. Comparison of important bond distances from XRD and theory.

	Compound 1		Compound 2	
Bonds	XRD	Theory	XRD	Theory
C17-O18	1.355	1.341	1.357	1.345
C17-C12	1.405	1.426	1.399	1.425
C12-C11	1.453	1.447	1.444	1.448
C11-N10	1.285	1.294	1.286	1.293
N9-N10	1.366	1.359	1.379	1.357

Hydrogen bonding by DFT calculation

The bond lengths, bond angles, dihedral angles, and hydrogen bond lengths calculated employing optimized geometry displays slight deviations as compared with the experimental (XRD) values (Tables 6 and 7). It is interesting to note that the intramolecular hydrogen bond length changes on comparison of compound **1** and **2**. The Mulliken charges on N10, O18, and H30 atoms of compounds **1** and **2** are presented in Table 6. In this table, as we move in the order of **1** to **2** the Mulliken charge on N10 and O18 becomes more negative, whereas on H30 becomes more positive. The electrostatic attraction between N10 and H30 increases in the compound **2** as compared to **1**. The hydrogen bond length decreases in molecule **2** as compared to **1** (Table 6). Thus, intramolecular charge transfer can be observed due to molecular rearrangement.

Conclusions

In summary, two *O*-hydroxy schiff bases, namely, *N*'-[(*Z*)-(2-hydroxy-4-methoxyphenyl) methylidene]pyridine-4-carbohydrazide and *N*'-[(*Z*)-(2-hydroxy-4-methoxyphenyl)methylidene]pyridine-3-carbohydrazide were synthesized by employing 2-hydroxy-4-methoxybenzaldehyde and isonicotic acid hydrazide and nicotinic acid hydrazide to address the effect of hydrazide moiety on the nature of hydrogen bonding attributes. The spectroscopic techniques, X-ray crystal structure determination as well as DFT calculations reveals that enolimine form of hydrogen bonding that is neutral hydrogen bonding is occurring and and hydrazide moiety behaves similar to a primary amine in the formation of *O*-hydroxy Schiff bases.

Acknowledgments

The authors are grateful to the Institution of Excellence, Vijnana Bhavana, University of Mysore, India, for providing the single-crystal X-ray diffractometer facility. The authors acknowledge Mr. Mukund for helping in acquisition of mass spectral data and Ms. Asha and Mr. Sanjay lal for IR data.

References

[1] Tidwell, T. T. (2008). *Angew. Chem. Int. Ed.*, *47*, 1016.
[2] Makal, A., et al. (2011). *Dalton Trans.*, *40*, 421.
[3] Chatziefthimiou, S. D., Lazarou, Y. G., Hadjoudis, E., Dziembowska, T., & Mavridis, I. M. (2006). *J. Phy. Chem. B*, *110*, 23701.
[4] Krol-Starzomska, A., Filarowski, M., Rospenk, I. & Koll, A. (2004). *J. Phys. Chem. A*, *108*, 2131.
[5] Dominiak, P. M., Grech, E., Barr, G., Teat, S., Mallinson, P. & Wozniak, K. (2003). *Chem. Eur. J.*, *9*, 963.
[6] Caulkins, B. G. et al. (2014). *J. Am. Chem. Soc.*, *136*, 12824.
[7] Metzler, C. M., Cahill, A., & Metzler, D. E. (1980). *J. Am. Chem. Soc.*, *102*, 6075.

[8] Vilanova, B. (2012). *J. Phys. Chem. A*, *116*, 1897.
[9] Filarowski, A., & Koll, A. (1998). *Vib. Spectrosc.*, *17*, 123.
[10] Nazir, H., Yildiz, M., Yilmaz, H., Tahir, M. N., & Ulku, D. (2000). *J. Mol. Struct.*, *524*, 241.
[11] Schilf, W., Kamienski, B., Szady-Chelmieniecka, A., & Grech, E. (2000). *Solid State NMR*, *18*, 97.
[12] Majerz, I., et al. (2000). *J. Mol. Struct.*, *552*, 243.
[13] Bruker. (2012). *SAINT PLUS*, Bruker AXS Inc.: Madison, Wisconsin, USA.
[14] Sheldrick, G. M. (2008). *Acta. Cryst., A64*, 112.
[15] Spek, A. L. (1990). *Acta. Cryst A*, *46*, C34.
[16] Macrae, C. F., et al. (2008). *J. Appl. Cryst.*, *41*, 466.
[17] Becke, D. (1993). *J. Chem. Phys.*, *98*, 5648.
[18] Becke, D. (1988). *Phys. Rev., A*, *38*, 3098.
[19] Lee, C., Yang, W. & Parr, R. G. (1988). *Phys. Rev.* B, *37*, 785.
[20] Dunning Jr., T. H. (1989). *J. Chem. Phys.*, *90*, 1007.
[21] Parr, R. G., & Weitao,Y. (1989). *Density-Functional Theory of Atoms and Molecules*, Oxford University Press: New York, USA.
[22] Kim, K., & Jordan, K. D. (1994). *J. Phy. Chem.*, *98*, 10089.
[23] Stephens, P. J., Devlin, F. J., Chabalowski, C. F., & Frisch, M. J. (1994). *J. Phy. Chem.*, *98*, 11623.
[24] Stevens, W. H., Basch, H., Krauss, M., & Jasien, P. (1992). *Can. J. Chem.*, *70*, 612.
[25] Cundari, T. R., & Stevens, W. J. (1993). *J. Chem. Phys.*, *98*, 5555.
[26] Hay, P. J., & Wadt, W. R. (1985). *J. Chem. Phys.*, *82*, 270.
[27] Dreuw, A., & Gordon, M. H. (2005). *Chem. Rev.*, *105*, 4009.
[28] Elliott, P., Furche, F., & Burke, K., (2009). *Rev. Comp. Chem.*, *26*, 91.
[29] Hirata, S., & Gordon, M. H., (1999). *Chem. Phy. Lett.*, *314*, 291
[30] Runge, E., & Gross, E. K. U. (1984). *Phys. Rev. Lett.*, *52*, 997.
[31] Casida, M. (1995). In: *Recent Advances in Density Functional Methods*, Chong, D. P. (Eds.), World Scientific: Singapore, Vol. 1, p. 155.
[32] Bauernschmitt, R., & Ahlrichs, R., (1996). *Chem. Phys. Lett.*, *256*, 454.
[33] Stratmann, R. E., Scuseria, G. E., & Frisch, M. J. (1998). *J. Chem. Phys.*, *109*, 8218.
[34] Furche, F., & Ahlrichs, R. (2002). *J. Chem. Phys.*, *117*, 7433.
[35] Furche, F., & Ahlrichs, R. (2004). *J. Chem. Phys.*, *121*, 12772.
[36] Li, H., Pomelli, C. S., & Jensen, J. H. (2003). *Theoret. Chim. Acta.*, *109*, 71.
[37] Li, H. (2009). *J. Chem. Phys.*, *131*, 184103.
[38] Wang, Y., & Li, H. (2010). *J. Chem. Phys.*, *133*, 034108.
[39] Schmidt, M. W., et al. (1993). *J. Comp. Chem.*, *14*, 1347.
[40] Gordon, M. S., & Schmidt, M. W. (2005). In: *Theory Applications of Computational Chemistry, the First Forty Years*, Dykstra, C. E., Frenking, G., Kim, K. S., Scuseria, G. E. (Eds.), Elsevier: Amsterdam, Chapter 41, p. 1167.